JOURNAL OF CATALYSIS **127**, 75–85 (1991)

Synthesis of Magnesium Oxide by the Sol–Gel Method: Effect of the pH on the Surface Hydroxylation

T. LOPEZ, I. GARCIA-CRUZ, AND R. GOMEZ

Universidad Autonoma Metropolitana-Ixtapalapa, Departamento de Quimica, A. P. 55-534, Ixtapalapa, Mexico D. F. 09340

Received August 23, 1989; revised February 20, 1990

Magnesium oxide was prepared by the sol–gel method. The method involves the hydrolysis of magnesium alkoxide in the presence of acid or basic catalysts followed by a polycondensation reaction. The synthesized solids were characterized by IR spectroscopy, X-ray diffraction, DTA, TGA, and electron microscopy. It is shown that the hydrolysis process depends on the catalyst's pH ($HCl > CH_3COOH > H_2C_2O_4 > H_2O > NH_4OH$). This effect can be explained by the reaction mechanism. The reaction is controlled by the hydrolysis at acid pH and by the polycondensation at a basic one. Solids prepared by this method are chemically homogeneous, very pure, and specifically hydroxylated. They can be widely used in the study of magnesium support effects in different catalytic reactions.

INTRODUCTION

Earlier studies have shown that metal catalysts supported on MgO behave quite differently from the ones supported on silica or alumina. The magnesia support effect is observed in catalytic activity, in selectivity, and in the formation of bimetallic particles. For benzene hydrogenation (*1*) and methylcyclopentane hydrogenolysis (*2*) on supported Ru catalysts, a high turnover value and a considerably smaller deactivation rate are reported for the Ru/MgO catalysts compared with Ru catalysts supported on SiO_2, Al_2O_3, or TiO_2. The MgO effect is also observed in the formation of bimetallic particles of Pt–Ru/MgO catalysts which are unusually enriched by Ru on their surface (*3*). Similar support effects have also been observed in Ru–Cu/MgO catalysts (*4*).

The particular behavior of this support is not completely understood. However, some reasons have been suggested: (i) magnesia stabilizes the metal in uncommon oxidation states (*5, 6*); (ii) its morphology and crystalline structure are easily modified (*7*); (iii) the occurrence of electronic transference between metal and support causes variations in the catalytic properties (*8*); and (iv) the acid strength of the hydroxyl groups found in the surface of the support is directly related to the catalytic activity (*9, 10*). It is evident that characterization of the MgO becomes necessary for its use and for interpretation of its effects when it is employed as a metal support.

MgO is obtained by thermal treatment of $Mg(OH)_2$ and $MgCO_3$. The oxide morphology depends on the preparation technique (calcination rate and temperature), but there is little information on the formation mechanism, especially on oxide hydroxylation.

In this work the method of synthesis known as sol–gel (*11*), which consists of hydrolysis and condensation of a magnesium alkoxide, is used. This method permits us to have different hydroxylated MgO precursors due to variations of pH in the reactive medium.

The homogeneity of a gel depends on the following parameters: the solubility of reactives in solvent, the sequence of addition of reactives, the temperature, and the pH of reaction.

The mechanism for obtaining a gel from a sol is probably a nucleophilic substitution.

0021-9517/91 $3.00

This is not clearly defined because it is difficult to separate the hydrolysis reaction from the polymerization; they occur almost simultaneously, forming the following intermediates: ethoxy (–Mg–OEt), hydroxy (–MgOH), and $Mg(OH)_2$ groups.

The reactions that occur are

Hydrolysis

$$Mg(OEt)_2 + H_2O \rightarrow Mg(OH)(OEt) + EtOH$$

$$Mg(OH)(OEt) + H_2O \rightarrow Mg(OH)_2 + EtOH$$

Condensation

$$-Mg-OEt + -Mg-OH \rightarrow -Mg-O-Mg- + EtOH$$

$$-Mg-OH + -Mg-OH \rightarrow -Mg-O-Mg- + H_2O$$

$$-Mg-OEt + -Mg-OEt \rightarrow -Mg-O-Mg + EtOEt$$

Ethanol acts as a solvent; it is obtained as a subproduct, and furthermore the quantity of alcohol present is involved in the reaction equilibrium.

The resultant gel is thermally treated at different temperatures, causing a dehydroxylation of the surface, until magnesium oxide is obtained. The dehydroxylation is studied by IR spectroscopy, DTA, TGA, and X-ray diffraction.

EXPERIMENTAL

Synthesis of $Mg(OEt)_2$. Mg (0.21 mole) is refluxed at constant agitation, with 1.7 moles of anhydrous ethylic alcohol and 3.9×10^{-4} mole of iodine. After 24 h of reaction, 6.82 mole of ethanol is added, continuing the reaction until all metallic magnesium has disappeared. The product is a white powder of magnesium ethoxide.

Synthesis of MgO gels. $Mg(OEt)_2$ (0.05 mole) is refluxed with 0.25 mole of H_2O and 0.85 mole of ethanol under constant agitation. After 10 min of reaction, a hydrolysis catalyst is added to the solution: (a) 0.02 mole of hydrochloric acid (pH 3); (b) 0.02 mole of acetic acid (pH 5); (c) 0.02 mole of oxalic acid (pH 5); (d) 0.02 mole of ammonium hydroxide (pH 9); (e) no catalyst (pH 7). The various solutions are kept at reflux and under constant agitation until they gel. The products obtained are dried at 70°C for 12 h and subsequently treated thermically at 300, 600, and 900°C for 72 h.

TABLE 1

Specific Surface Area (m^2/g) for Different Solids as a Function of pH and Calcination Temperature

Temperature (°C)	HCl pH 3	CH_3COOH pH 5	$H_2C_2O_4$ pH 5	No catalyst pH 7	NH_4OH pH 9
300	44.48	24.19	35.60	—	67.90
600	—	15.40	18.50	29.80	31.21
900	6.40	2.60	11.80	12.40	14.60

CHARACTERIZATION

Solids were studied by IR spectroscopy in a Nicolet MX-1 unit, using pellets of KBr. To avoid a possible reaction between the KBr and the MgO during the thermal treatments, the pellets were prepared with MgO samples previously heated for 72 h at different temperatures (300, 600, and 900°C). Possible rehydroxylation of the MgO surface did not occur in our cell since the IR spectra obtained are the same as those in the case of pure MgO pellets; however, the transmittance under these conditions was very poor. A Shimadzu analyzer and a Siemens diffractometer were used for DTA and TGA and for X-ray diffraction, respectively.

The BET areas were determined in a Perkin–Elmer sorptometer with N_2 adsorption at 77.5 K. The surface areas for the various catalysts are reported in Table 1, where temperature and pH effects can also be observed. Micrographs were obtained with a scanning Phillips microscope.

RESULTS AND DISCUSSION

Infrared Spectroscopy

IR vibrations associated with the hydroxyl group produce several absorption

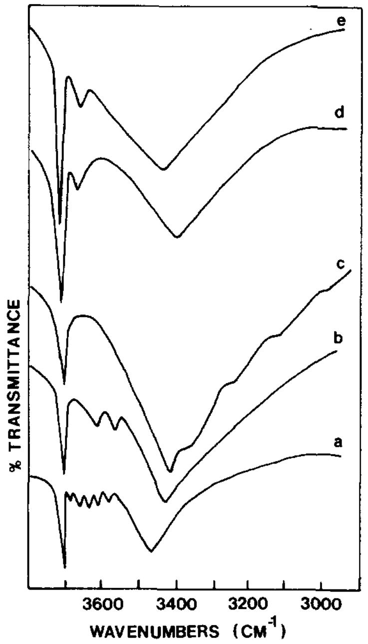

FIG. 1. IR spectra of MgO gels synthetized at pH (a) 3 (HCl); (b) 5 (CH_3COOH); (c) 5 ($H_2C_2O_4$); (d) 7 (H_2O); (e) 9 (NH_4OH).

bands, which are separable in the region 4000 to 3000 cm^{-1}. Kirklin *et al.* (*12*) established the existence of eight absorption peaks in this region and they ascribed them to the OH groups that are found, in different forms, in the magnesia surface.

At 3699 cm^{-1}, a narrow and intense band, associated to an OH frequency that does not form an hydrogen bond, appears in all gels (Fig. 1). In MgO synthesis by the sol–gel process, hydrolysis is improved by the presence of acid and basic catalysts, leading to $Mg(OH)_2$ formation that persists after the gelation. Kirklin *et al.* (*12*) attributed it to a precipitation of $Mg(OH)_2$ in the oxide; this idea was further supported by Glass and Searle (*13*) and Sibley *et al.* (*14*).

When gels are prepared at pH 3, five peaks are observed at 3682, 3652, 3624, 3603, and 3574 cm^{-1}, due to the existence of species with weak hydrogen bonds which absorb between 3640 and 3500 cm^{-1}. The primary hydroxyl groups that form hydrogen bonds absorb in the limit of higher frequency of this region (3640 cm^{-1}); as the bond between oxygen and hydrogen progressively weakens, peaks appear at lower frequencies (Fig. 1a). Aelion *et al.* (*15*) find that when a metallic alkoxide is catalyzed by HCl, hydrolysis is favored as acid concentration in the reaction increases. In this work, the amount of HCl added will permit a totally hydroxylated surface after MgO formation, and is due to the appearance of the aforementioned five bands; this phenomenon is not observed when the pH of the reaction is increased.

At 3475 cm^{-1}, a wide intense band exists, associated to OH vibration due to H_2O in the air.

When the pH is increased to 5 with acetic acid, the number of peaks in this region decreases (Fig. 1b), and only vibrations at 3605, 3563, and 3444 cm^{-1} are found. These bands are shifted to lower wavenumbers because weaker hydrogen bonds are established. At a lower H^+ concentration that catalyzes the hydrolysis reaction, the result is an oxide with a partially hydroxyled surface. However, when the catalyst is oxalic acid, the band of free OH weakens and new bands appear at lower frequencies, which indicates the existence of vacancies in MgO. In Fig. 1c two peaks are observed, at 3412 and 3371 cm^{-1}. This separation of the band in two occurs only when the oxalate ion is involved, since it behaves as a strong ligand and becomes complexed in the oxide network. The oxalate coordinates with the metal and vacancies are produced. As evidence of this coordination, characteristic bands of carbonyl groups appear at 1671 and 1646 cm^{-1} and are shifted toward low frequency regions (Fig. 5). When the carbonyl group is coordinated, the absorption of CO is shifted toward low frequency, because it tends to diminish the double bond character. However, in the pure oxalic acid, the band appears at 1700 cm^{-1}.

At pH 7, the OH peak intensity increases, and another one appears at 3649 cm^{-1}. The

3384 cm^{-1} peak related to the OH in the surface absorption at 3384 cm^{-1} is observed (Fig. 1d), because few OH exist united to the surface.

When the reaction occurs at pH 9, a nucleophilic substitution takes place to form -MgO$^-$ species. Condensation occurs more rapidly than hydrolysis, and therefore partially hydrolyzed monomers are polymerized. The reaction occurs more often among protonated species than among nonprotonated ones.

$$\text{-MgO}^- + \text{HO-Mg-} \rightarrow \text{-Mg-O-Mg-} + \text{OH}^-$$

The surface of the product will be slightly hydroxylated and the solid will have an appreciable quantity of H_2O and organic groups included in its structure. In the IR spectrum, bands at 3699, 3643, and 3419 cm^{-1} are observed (Fig. 1e).

Effect of Temperature on the Dehydroxylation Process

Mineral acids, such as HCl, are particularly effective in catalyzing hydrolysis reactions of metallic alkoxides by an exothermic process that increases the reaction temperature and reduces the condensation rate. For this reason, there is a large quantity of OH groups in the product. It has been shown that the terminal OH united to the network are more acidic than those placed in the center of the polymeric chain (*16, 17*).

The IR spectra of oxides obtained at pH 3 and thermally treated at different temperatures are shown in Fig. 2.

At 300°C the number of peaks in the OH region decreases, and only one peak is observed at 3402 cm^{-1} with a small shoulder at 3623 cm^{-1}. At 600°C, this band is displaced toward higher frequencies (3410 cm^{-1}) and its intensity decreases. When the solid is treated at 900°C there is no absorption in this region, which indicates that the MgO has been totally dehydroxylated. At low temperatures the characteristic OH flexion peak appears (1622 cm^{-1}) due to the water in the air and hydroxyl groups on the surface. This peak is not present at high temperatures.

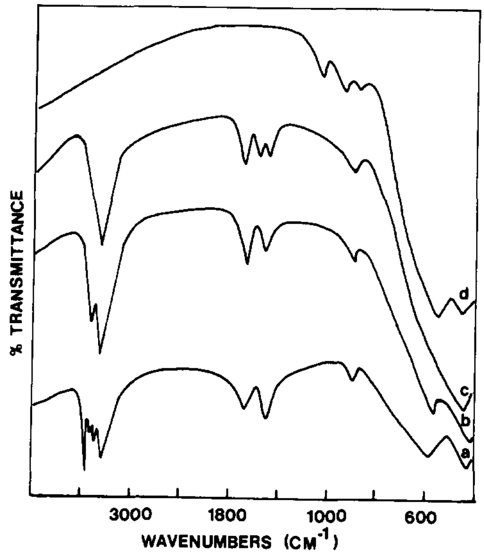

FIG. 2. IR spectra of MgO gels synthetized at pH 3 with HCl treated at (a) room temperature; (b) 300°C; (c) 600°C; and (d) 900°C.

In these solids, very few ethoxy groups are tied to the network. For this reason, a low-intensity band, typical of a symmetrical C–H deformation, appears at 1433 cm^{-1}. Due to the proximity of stretching ethylene bands and the ethyl asymmetrical stretching ones, only one band is observed; however, at 600°C it divides into two bands (1482 and 1417 cm^{-1}), which disappear at 900°C.

Below 1000 cm^{-1}, two vibration bands of the Mg–O bond appear in a rather undefined manner, and are accompanied by a wide band when the temperature increases because in ionic solids such as magnesium oxide, individual ion vibration is caused by the displacement of these ions with respect to those ions nearest to them. The resulting spectral bands are wide and are observed every time at lower energies, due to the effect of the weight of the metallic ion.

At basic pH, hydrolysis is inhibited, increasing the polymerization rate (Table 2). A large number of ethoxy groups are present in the final solid and the acidity of protons

TABLE 2

Effect of the Catalyst on the Gelation Time

	HCl	CH_3COOH	$H_2C_2O_4$	No catalyst	NH_4OH
pH	3	5	5	7	9
Gelation time (h)	89	48	67	70	21

tied to the magnesia is increased as the basicity of the other bounded groups decreases (Fig. 3).

In the region 3000 to 4000 cm^{-1}, the effect is similar to the former case. At 300°C, a single absorption appears at 3410 cm^{-1} and decreases in intensity as the temperature increases. This band disappears at 900°C.

Former studies support the idea that when organic substances exist in the synthesis, it is possible to find radicals tied to the surface (*19*, *20*), causing vacancies in the oxide. As a consequence, two bands of high intensity are observed at 1491 and 1433 cm^{-1}, differing from the sample prepared with HCl, in which only a small band appears. It is very important to note that interactions in the surface affect both the position and the intensity of the peaks. The ethylene group has two stretching vibrations: one symmetrical and the other an asymmetrical deformation. The stretching vibrations noted above are also observed.

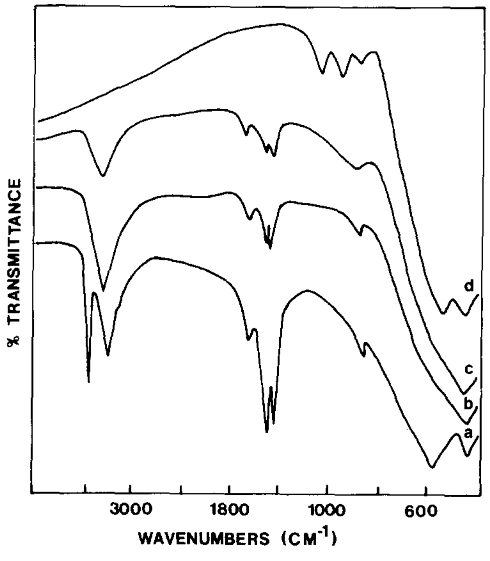

FIG. 3. IR spectra of MgO gels obtained at pH 9 with NH_4OH treated at (a) room temperature; (b) 300°C; (c) 600°C; and (d) 900°C.

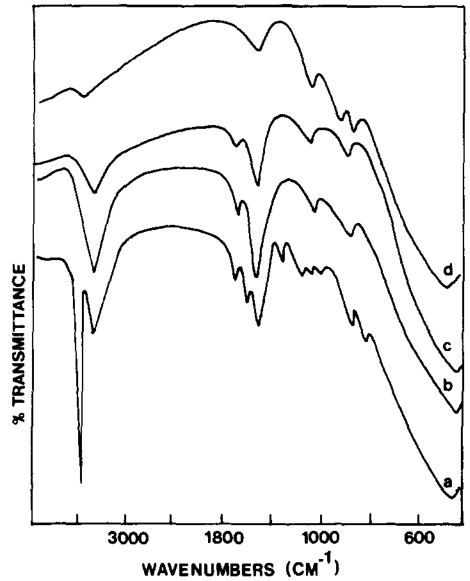

FIG. 4. IR spectra of MgO gels synthetized at pH 7 and treated at (a) room temperature; (b) 300°C; (c) 600°C; and (d) 900°C.

It is evident that these organic groups will be desorbed as the temperature increases; hence, the number of vacancies decreases. This leads to structural rearrangements in the oxide, due to the thermal treatment. At 300°C, the peaks are shifted toward lower frequencies and their intensity decreases, until at 900°C only the typical MgO bands are observed.

When the pH of the reaction is 7 (Fig. 4), the gelling time increases relative to the catalyzed reaction by bases. The IR spectra of these samples are comparable to those obtained at pH 9; the only difference is that at 900°C a band is still observed at 3435 cm^{-1}, which suggests that the surface has not been totally dehydroxyled at that temperature. However, when the reaction is

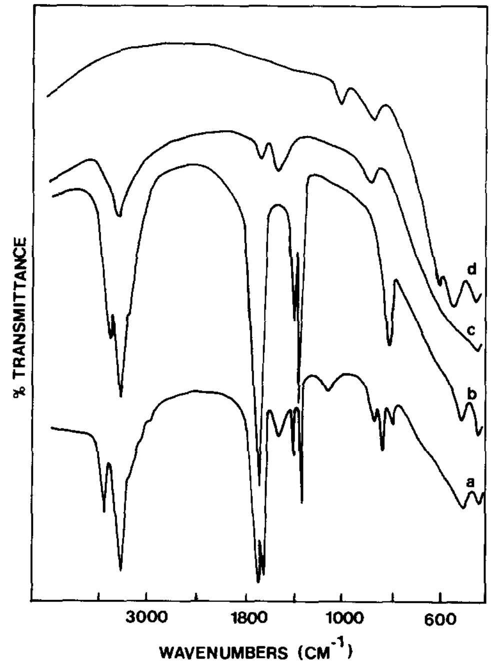

FIG. 5. IR spectra of MgO gels synthetized at pH 5 with $H_2C_2O_4$ treated at (a) room temperature; (b) 300°C; (c) 600°C; and (d) 900°C.

catalyzed by carboxylic acids, there is a different effect in the OH absorption region. When the reaction is catalyzed by oxalic acid (Fig. 5) and the product is thermally treated at 300°C, the three bands between 3200 and 2960 cm^{-1} caused by OH vacancies disappear. Only a small shoulder at 3180 cm^{-1} remains and is assigned to a simple vacancy (*13*). In addition, a strong absorption peak appears at 3410 cm^{-1}, accompanied by a small peak at 3582 cm^{-1}, indicating that at this temperature part of $Mg(OH)_2$ still exists, precipitated in the MgO. When the sample is treated at 600°C, the vacancy peaks no longer exist and the one at 3410 cm^{-1} diminishes in intensity. At 900°C there is no absorption in this region, which indicates that the magnesium oxide is entirely dehydroxylated (Fig. 5).

When acetic acid is used (Fig. 6) in the support preparation and the product is heated at 300°C, two intense peaks are observed at 3632 and 3402 cm^{-1} and persist even at 600°C. In this case, the amount of $Mg(OH)_2$ contained in the oxide does not decompose under the thermal treatment. In some way the acetic acid appears to be stabilizing the hydroxide. Between those two bands a third one should appear at 3595 cm^{-1}, due to a stretching vibration of the carboxylic acid O–H. However, no band exists in this region for this case.

In both cases, with oxalic and acetic preparations, intense absorptions appear between 1700 and 1500 cm^{-1} caused by symmetrical and asymmetrical vibrations of the carbonyl groups. A band is present at 1031 cm^{-1} (acetic acid) or at 1097 cm^{-1} (oxalic acid), due to a vibration outside of the OH plane on the acids.

Between 1450 and 1260 cm^{-1} typical carbon–hydrogen stretching vibration bands are observed. All of these bands disappear when the sample is heated. At 300°C the number of bands is reduced, but the carbonyl group intensity remains nearly con-

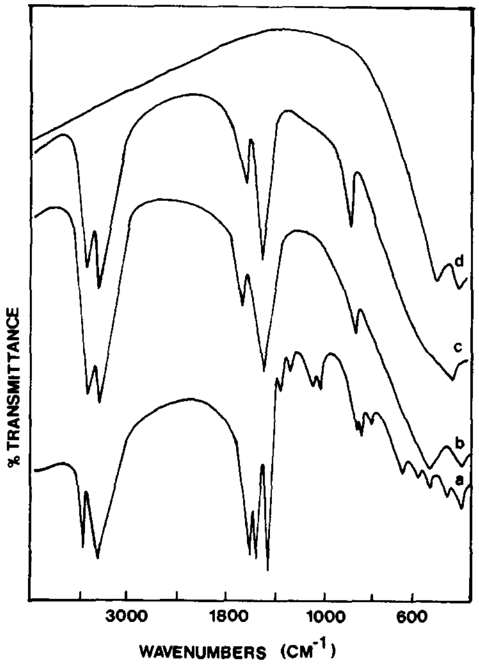

FIG. 6. IR spectra of MgO gels synthetized at pH 5 with CH_3COOH treated at (a) room temperature; (b) 300°C; (c) 600°C; and (d) 900°C.

FIG. 7. Thermogram of MgO obtained at pH 3 (HCl).

stant. At 600°C the C–H stretching bands are no longer observable and those of the carbonyl group have almost disappeared. At 900°C there is no absorption in this region, and only the Mg–O vibrations can be observed.

TGA and DTA of MgO Gels Synthesized at Different pH

pH 3. The endothermic peak observed at 110°C (Fig. 7) is attributed to vaporization of water and ethylic alcohol physically absorbed in the solid. A second endothermic peak appears at 190°C, which is due to vaporization of alkoxy residual groups as well as to desorption of OH groups that are more weakly tied to the solid.

At 370 and 435°C, two more peaks which are caused by the total dehydroxylation of MgO appear. This oxide undergoes two equally important weight changes, the first one being 19.4% and the second one 26%. The latter occurs in a temperature range from 200 to 540°C. These results are in agreement with the infrared ones. At these temperatures the most surface structure transformations occur (Fig. 2).

pH 5. As previously mentioned, this pH was obtained by using two different carboxylic acids. When acetic acid is used as the hydrolysis catalyst, a pronounced endothermic peak appears in the thermogram at 145°C, accompanied by a small shoulder at 228°C. However, when the catalyst is oxalic acid, the first endothermic peak is displaced to 165°C and its size diminishes almost completely. The other peak increases and is observed at 225°C (Figs. 8 and 9). In one case, great quantities of water and ethanol are occluded in gel, whereas in the other, there is an excess of residual alkoxy and a great desorption of organic groups and carbonyls. At approximately 350 and 500°C, there are two endothermic peaks due to surface dehydroxylation. In TGA, two weight losses are seen (15.5 and 34.9%) for gels synthetized with acetic acid and three in gels obtained with oxalic acid (17.8, 15.34, and 23.01%), due to the loss of two different carbonyl groups.

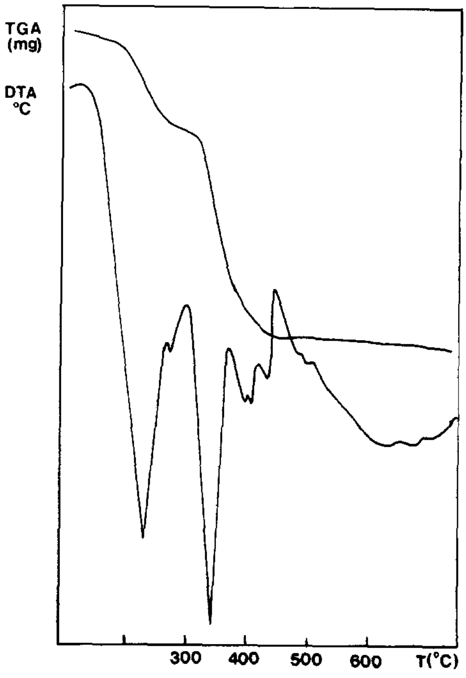

FIG. 8. Thermogram of MgO obtained at pH 5 (CH$_3$COOH).

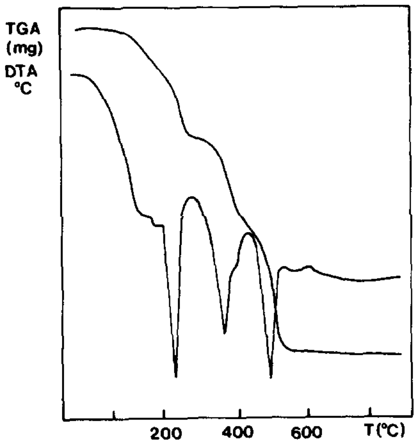

FIG. 9. Thermogram of MgO obtained at pH 5 ($H_2C_2O_4$).

pH 7. At this pH value an interesting phenomenon occurs: most of the peaks observed in former thermograms disappear. Only a small endothermic peak at 185°C, which is accompanied by a weight loss of 3.14%, and another peak at 375°C with a loss of 28.79% remain (Fig. 10).

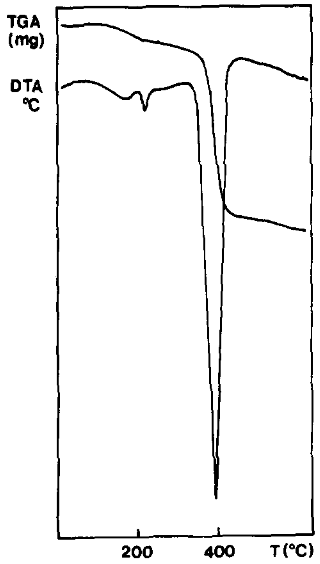

FIG. 10. Thermogram of MgO obtained at pH 7 (H_2O).

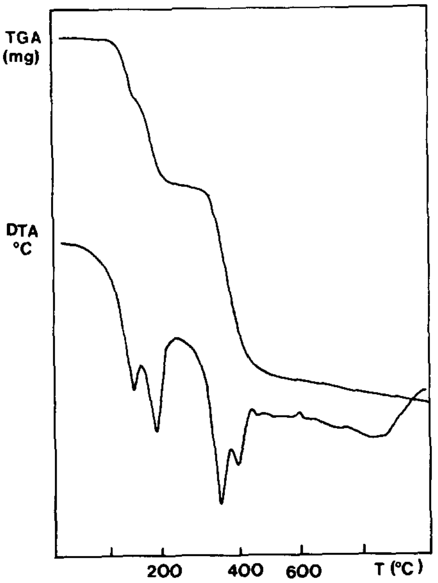

FIG. 11. Thermogram of MgO obtained at pH 9 (NH_4OH).

Gelation reactions do not occur in a basic medium and, therefore, hydrolysis is affected. This leads to an increase in the condensation or polymerization rates. In this case, a lesser quantity of H_2O will be occluded in the solid and a larger quantity of organic residues will be retained. These residues carbonize at approximately the same dehydroxylation temperature, causing the large peak at 375°C. The small quantity of superficial OH groups in this sample results in the disappearance of the 500°C peak observed in the other cases.

pH 9. The mechanism of nucleophilic substitution that occurs at this pH value results in the formation of ethanol in the reaction equilibrium. This ethanol desorbs at 129°C, producing a small endothermic peak. In this case, most of the reactants have been converted and very few residual alkoxy groups are carbonized at 242°C. At 590°C two endothermic peaks, characteristic of dehydroxylation, are observed (Fig. 11).

MORPHOLOGY OF THE MgO

Several authors have found that the support textural and structural properties can influence the metal phase catalytic behavior (*21–23*). As is well known, the final state of a support is strongly dependent upon the method of preparation. The specific areas of the samples were measured in the usual way using the BET equation in Perkin–Elmer sorptometer equipment. Table 1 shows the area values as a function of pH, synthesis, and calcination temperature.

The maximum area obtained is 68 m^2/g for a gel treated at 300°C and synthesized using NH_4OH as a catalyst. This higher area compared to the other samples is due to the residual organic groups which represent a much bigger volume than the hydroxyls. The smaller areas at acid pH values are due to the inverse phenomenon.

X-ray diffraction patterns of samples treated at 900°C are identical in all cases and show three peaks characteristic of MgO [d: $2.11_x^{(111)}$, $1.49_y^{(011)}$, $1.22_1^{(001)}$] with the exception of the support prepared at pH 7. The

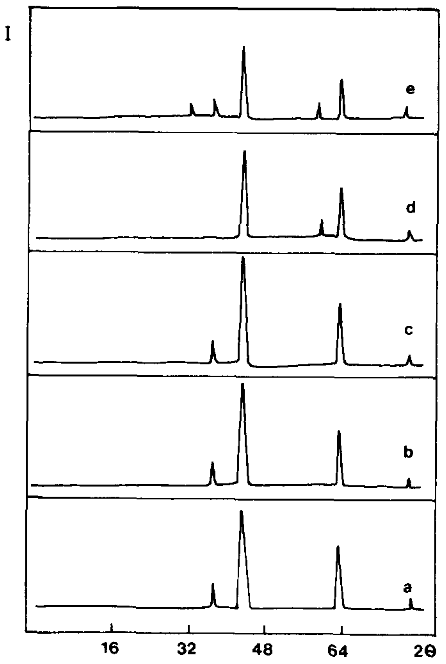

FIG. 13. X-ray diffraction patterns of MgO treated at 900°C obtained at pH (a) 3 (HCl); (b) 5 (CH_3COOH); (c) 5 ($H_2C_2O_4$); (d) 7; and (e) 9 (NH_4OH).

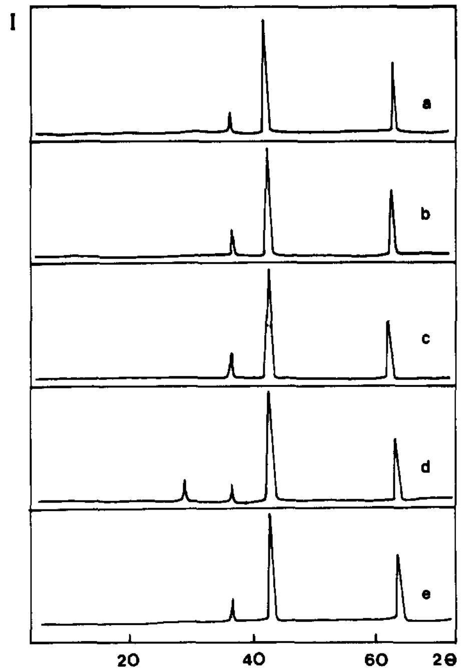

FIG. 12. X-ray diffraction patterns of MgO treated at 600°C obtained at pH (a) 3 (HCl); (b) 5 (CH_3COOH); (c) 5 ($H_2C_2O_4$); (d) 7; and (e) 9 (NH_4OH).

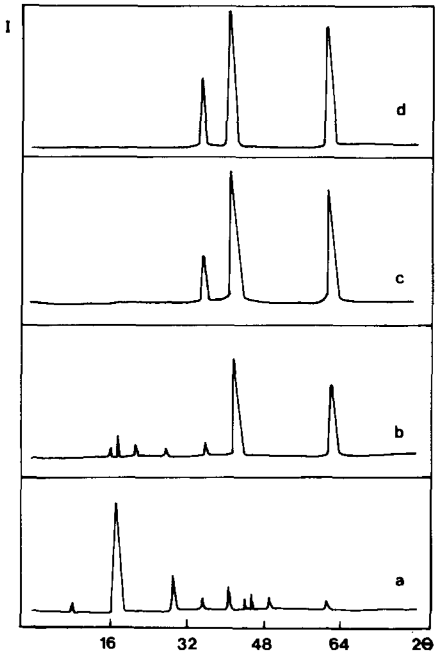

FIG. 14. X-ray diffraction patterns of MgO synthesized at pH 5 with oxalic acid and treated at (a) room temperature; (b) 300°C; (c) 600°C; and (d) 900°C.

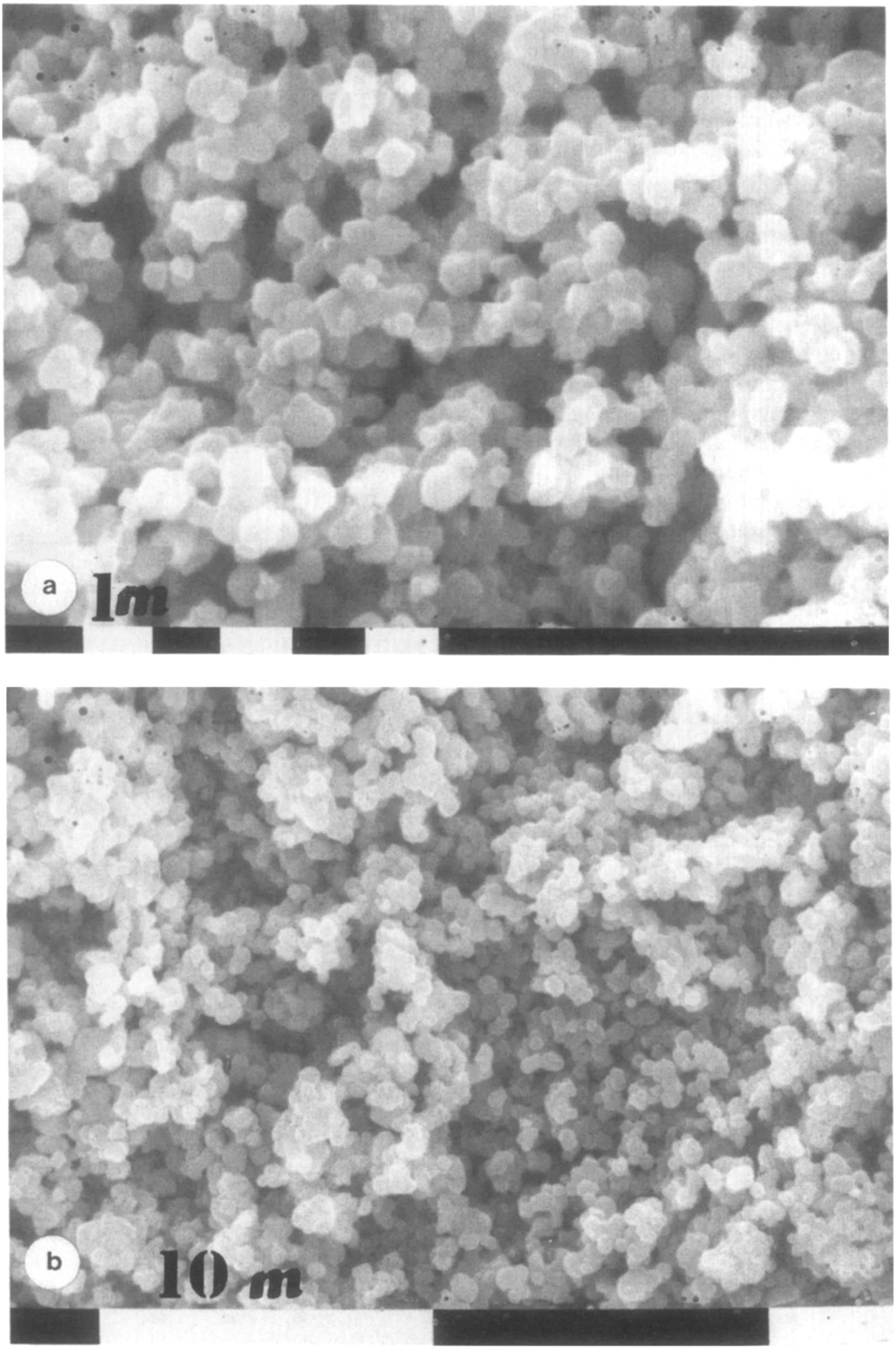

FIG. 15. Scanning electron microscopy of MgO treated at 900°C: (a) pH 3 (HCl) and (b) pH 5 (CH_3COOH).

peaks presented in this case are identified as $Mg(OH)_2$ brucite type, which is indicative of a surface not completely dehydroxylated (Fig. 12). These results are in agreement with the infrared study.

In Fig. 13 (900°C) the X-ray diffraction patterns show an increase of crystal size in terms of calcination temperature compared with the diffraction pattern at 600°C (Fig. 12). Similar spectra are likewise observed for the samples at pH 3, 5, and 9. A singular case is that of the X-ray spectra of the samples prepared with oxalic acid (Fig. 14). In this case at room temperature the characteristic MgO lines are not observed. Under these conditions the whole product is an amorphous xerogel. However, it shows MgC_2O_4 peaks at d 3.96_x, 5.18_8, and 2.42_8, because at this temperature, the oxalate is tied to the MgO, as discussed above. When xerogel is treated at 300°C, small peaks typical of MgO appear in addition to those caused by $Mg(OH)_2$ brucite type, and cause those of magnesium oxalate to disappear. At 900°C only the MgO peaks are observed and as before, the size of the crystal increases with temperature of treatment.

The pH at which synthesis is performed does not produce significant changes in morphology of MgO. In Fig. 15, the micrographs of the oxides prepared at pH 3 and 5 are shown. In both cases the same morphology is present and small cubic crystals can be observed.

CONCLUSIONS

The importance of the present article lies in establishing that MgO supports can be obtained by the sol–gel method at controlled pH, resulting in specifically hydroxylated samples. They can be used in studying the effects of the support on metallic catalytic activity, with the advantage of having supports that are free of residual impurities commonly present in the raw materials usually employed in traditional processes. The effects of these MgO supports on catalytic activity will be dealt with in future work.

ACKNOWLEDGMENTS

We acknowledge CONACyT-CONICET Mexico–Argentina and CYTED-D PROGRAM for financial support.

REFERENCES

1. Viniegra, M., Gomez, R., and Gonzalez, R. D., *J. Catal.* **111,** 429 (1988).
2. Villamil, P., Reyes, J., Rosas, N., and Gomez, R., *J. Mol. Catal.* **54,** 205 (1989).
3. Del Angel, G., Medina, C., Gomez, R., Rejai, B., and Gonzalez, R. D., *Catal. Today* **5,** 395 (1989).
4. Galvagno, S., Schwank, J., Parravano, G., Garbassi, F., Marzi, A., and Tauszick, G. R., *J. Catal.* **69,** 283 (1981).
5. Schwank, J., Galvagno, S., and Parravano, G., *J. Catal.* **63,** 415 (1980).
6. Driessen, J. M., Poels, E. K., Hindermann, J. P., and Ponec, V., *J. Catal.* **82,** 26 (1983).
7. Modie, A. F., and Warble, C., *J. Cryst. Growth.* **74,** 89 (1986).
8. Logan, A. D., and Datye, A. K., *J. Catal.* **112,** 595 (1988).
9. Lercher, J. A., and Noller, H., *J. Catal.* **77,** 152 (1982).
10. Ward, J. W., *J. Catal.* **9,** 225 (1967).
11. Klein, L. C., *Ann. Rev. Mat. Sci.* **15,** 227 (1985).
12. Kirklin, P. W., Auzins, P., and Wertz, J. E., *J. Phys. Chem. Solids* **26,** 1067 (1965).
13. Glass, A. M., and Searle, T. M., *J. Chem. Phys.* **46,** 2092 (1967).
14. Sibley, W. A., Nelson, C. M., and Chen, Y., *J. Chem. Phys.* **48,** 4582 (1968).
15. Aelion, R., Loebel, A., and Eirich, F., *J. Amer. Chem. Soc.* **72,** 5705 (1950).
16. Brinker, C. J., Keefer, K. D., Schaefer, D. W., and Ashley, C. S., *J. Non-Cryst. Solids.* **48,** 47 (1982).
17. Brinker, C. J., Keefer, K. D., Schaefer, D. W., Assink, R. A., Kay, B. D., and Ashley, C. S., *J. Non-Cryst. Solids.* **63,** 45 (1984).
18. Hair, M. L., and Hertl, W., *J. Phys. Chem.* **74,** 91 (1970).
19. Smith, D. R., and Tench, A. J., *Chem. Commun.,* 1113 (1968).
20. Tench, A. J., and Holroyd, P., *Chem. Commun.,* 471 (1968).
21. Shastri, A. G., Chae, H. B., Bretz, M., and Schwank, J., *J. Phys. Chem.* **89,** 3761 (1985).
22. Dash, J. G., Ecke, R. S. J., Vilches, O. E., and Whittermore, O., *J. Phys. Chem.* **82,** 1450 (1978).
23. Leofanti, G., Solari, M., Tauszik, G. R., Garbassi, F., Galvagno, S., and Schwank, J., *Appl. Catal.* **3,** 131 (1982).